Phosphorylation of multiple sites within an acidic region of Alcadein α is required for kinesin-1 association and Golgi exit of Alcadein α cargo

Yuriko Sobu[a], Keiko Furukori[a,b], Kyoko Chiba[a], Angus C. Nairn[b], Masataka Kinjo[c], Saori Hata[a], and Toshiharu Suzuki[a,*]

[a]Laboratory of Neuroscience, Graduate School of Pharmaceutical Sciences, Hokkaido University, Sapporo 060-0812, Japan; [b]Department of Psychiatry, Yale University School of Medicine, New Haven, CT 06508; [c]Laboratory of Molecular Cell Dynamics, Faculty of Advanced Life Science, Hokkaido University, Sapporo, 001-0021, Japan

ABSTRACT **Alcadein α (Alcα) is a major cargo of kinesin-1 that is subjected to anterograde transport in neuronal axons. Two tryptophan- and aspartic acid-containing (WD) motifs located in its cytoplasmic domain directly bind the tetratricopeptide repeat (TPR) motifs of the kinesin light chain (KLC), which activate kinesin-1 and recruit kinesin-1 to Alcα cargo. We found that phosphorylation of three serine residues in the acidic region located between the two WD motifs is required for interaction with KLC. Phosphorylation of these serine residues may alter the disordered structure of the acidic region to induce direct association with KLC. Replacement of these serines with Ala results in a mutant that is unable to bind kinesin-1, which impairs exit of Alcα cargo from the Golgi. Despite this deficiency, the compromised Alcα mutant was still transported, albeit improperly by vesicles following missorting of the Alcα mutant with amyloid β-protein precursor (APP) cargo. This suggests that APP partially compensates for defective Alcα in anterograde transport by providing an alternative cargo receptor for kinesin-1.**

Monitoring Editor
Kozo Kaibuchi
Nagoya University

Received: May 17, 2017
Revised: Sep 18, 2017
Accepted: Oct 26, 2017

INTRODUCTION

Axonal transport in neurons is largely mediated by microtubule-associated motor proteins such as kinesin superfamily proteins (KIFs) for anterograde transport and dynein for retrograde transport (reviewed in Hirokawa *et al.*, 2010). Kinesin-1/conventional kinesin, the first anterograde molecular motor to be identified (Vale *et al.*, 1985), is a heterodimer composed of two kinesin heavy chains (KHC/KIF5) and two kinesin light chains (KLC) (reviewed in Verhey and Hammond, 2009). KHC includes a microtubule-binding motor domain with ATPase activity, and KLC has a tetratricopeptide repeat (TPR) domain that interact with cargo and cargo-mediating adaptor proteins. When kinesin-1 is not associated with cargo, it exists in an auto-inhibited state without microtubule-binding ability (Verhey *et al.*, 1998).

Alcadein/calsyntenin family proteins (Alcα/Clstn1, Alcβ/Clstn3, and Alcγ/Clstn2) are neuronal type I membrane proteins that are subject to proteolytic processing, primarily by ADAM10/17, to generate a membrane-associated carboxy-terminal fragment (Alc CTF) and a secreted amino-terminal region (sAlc). The Alc CTF is then subjected to secondary cleavage within its membrane-spanning region by the γ-secretase complex (Hintsch *et al.*, 2002; Araki *et al.*, 2003, 2004; Hata *et al.*, 2009; Piao *et al.*, 2013), as is amyloid β-protein precursor (APP), to generate an intracellular cytoplasmic domain fragment (Alc ICD) and to secrete a nonaggregation-prone p3-Alc peptide that is involved in the pathology of Alzheimer's disease (AD) (Hata *et al.*, 2011, 2012; Konno *et al.*, 2011; Kamogawa *et al.*, 2012; Omori *et al.*, 2014).

The cytoplasmic domain of Alc proteins contains one or two KLC-binding tryptophan- and aspartic acid-containing (WD) motifs, with which the tetratricopeptide repeat (TPR) motifs of KLC interact

This article was published online ahead of print in MBoC in Press (http://www.molbiolcell.org/cgi/doi/10.1091/mbc.E17-05-0301) on November 1, 2017.

The authors declare no conflict of interest.

Author contributions: Y.S., S.H., A.C.N., and T.S. participated in the design of the study, and Y.S. and K.F. carried out all studies; K.Y. and M.K. participated in TIRF analysis, and S.H. participated in MS analysis and antibody preparation; Y.S. and T.S. conceived the study, and Y.S., S.H., A.C.N., and T.S. wrote the paper. All authors read and approved the final manuscript.

*Address correspondence to: Toshiharu Suzuki (tsuzuki@pharm.hokudai.ac.jp).

Abbreviations used: AD, Alzheimer's disease; Alcα, Alcadein α; APP, amyloid precursor protein; GFP, green fluorescent protein; KHC, kinesin heavy chain; KLC, kinesin light chain; TPR, tetratricopeptide repeat; WD motif, tryptophan and aspartic acid–containing sequence.

with high affinity (Araki *et al.*, 2007; Dodding *et al.*, 2011). Interestingly, the short WD motif can activate kinesin-1 in a KLC1-dependent manner (Kawano *et al.*, 2012; Yip *et al.*, 2016). Among the three Alc proteins, Alcα predominantly functions as a cargo receptor for kinesin-1. Vesicles harboring Alcα functionally associated with kinesin-1 transport various cargo substances. Alcβ appears to have acquired other functions during evolution (Pettem *et al.*, 2013; Um *et al.*, 2014; Wang *et al.*, 2014), and Alcβ can also interact with kinesin-1 (Kawano *et al.*, 2012). Alcγ expression may be lower in adults than expression of Alcα and Alcβ (Hata *et al.*, 2011), but Alcγ also binds kinesin-1 and may be involved in memory performance and cognition (Boraxbekk *et al.*, 2015; Lipina *et al.*, 2016).

Alcα is reported to function as a cargo receptor when associated with kinesin-1 (Araki *et al.*, 2007). Either WD motif of Alcα can bind KLC1 TPR domains, and one TPR domain is able to bind two WD motifs (Zhu *et al.*, 2012). This property is thought to generate a strong interaction between Alcα and KLC with the high affinity needed to transport vesicles containing Alcα associated with kinesin-1, the Alcα cargo, in long neuronal axons (Kawano *et al.*, 2012).

Alcα forms a tripartite complex with APP mediated by cytoplasmic interaction with X11L predominantly in Golgi, and Alcα and APP cargoes are subject to respective independent anterograde transport, generally following Golgi exit (Araki *et al.*, 2003, 2004, 2007; Takei *et al.*, 2015). However, the molecular regulation of the Golgi exit of Alcα and APP remains unclear. Furthermore, an acidic region, which resides between WD1 and WD2 in the Alcα cytoplasmic region, was predicted to be intrinsically disordered by the PONDR-FIT prediction tool (Xue *et al.*, 2010a), but the role of this large acidic region in the function and/or metabolism of Alcα has not been revealed.

Together with Alcα, other membrane proteins including APP, apolipoprotein E receptor 2 (ApoER2), and a neural cell adhesion molecule (NCAM) are also known to serve as cargo and/or cargo receptors for kinesin-1 in neurons (Koo *et al.*, 1990; Kamal *et al.*, 2000; Araki *et al.*, 2007; Verhey *et al.*, 2001; Chiba *et al.*, 2014a; Wobst *et al.*, 2015). However, it remains controversial how the interaction between cargo receptors and kinesin-1 is regulated during the various stages of cargo transport, including during vesicular cargo formation at the Golgi, transportation in axons, and release in the nerve terminal. Previous reports suggest that phosphorylation of kinesin-1 and/or adapter proteins mediate the association of the cargo receptor with KLC, thereby regulating cargo binding to the motor, or motor activity directly (Chua *et al.*, 2012; Xu *et al.*, 2012; Fu and Holzbaur, 2013). A report has also suggested that association of Alcα with KLC1 is regulated by phosphorylation of KLC1 (Vagnoni *et al.*, 2011).

In the present study, we found that the cytoplasmic domain of Alcα is phosphorylated at multiple serine residues in the acidic region, and phosphorylation is required for a strong association with KLC. When unphosphorylated, Alcα fails to exit efficiently from the Golgi, and is missorted into other transport vesicles such as APP cargo vesicles, which partially compensates for the failure of defective Alcα to facilitate Golgi exit. The present results reveal the functional importance of Alcα phosphorylation at multiple sites in regulating the transport of Alcα cargo by kinesin-1 and the proper formation of post-Golgi Alcα cargo.

RESULTS

Phosphorylation of the Alcα cytoplasmic region is required for association with KLC

The cytoplasmic domain of Alcα binds directly to KLCs and includes putative phosphorylatable amino acid residues that may regulate the interaction with KLCs. We first investigated whether the cytoplasmic domain of Alcα was subject to phosphorylation in vivo using membrane and cytoplasmic fractions of mouse brain homogenates. Alcα CTF (Alcα$^{816–971}$), a carboxyl-terminal fragment generated by primary cleavage of Alcα, was detected in the membrane fraction, and Alcα ICD (Alcα$^{868–971}$ as major and Alcα$^{871–971}$ as minor products), a fragment endogenously generated by cleavage of Alcα CTF by γ-secretase, was recovered from the cytoplasmic fraction following immunoprecipitation and detected by immunoblotting using an anti-Alcα antibody (Figure 1A; Araki *et al.*, 2004; Hata *et al.*, 2009; Piao *et al.*, 2013). Interestingly, both endogenous fragments generated from Alcα in vivo migrated faster by gel electrophoresis following dephosphorylation with lambda protein phosphatase (λPPase). These results suggest that Alcα is a neuronal phosphoprotein that is phosphorylated within the cytoplasmic region in vivo.

We next confirmed phosphorylation of the cytoplasmic domain of Alcα in cells by prelabeling with [^{32}P] orthophosphate. HEK293 cells expressing the Alcα intracellular domain fragment (Alcαcyt, amino acid residues 871–971) were radiolabeled with [^{32}P]orthophosphate, and Alcαcyt was isolated from cell lysates by immunoprecipitation with anti-Alcα antibody to analyze phosphorylation by autoradiography, while protein expression was assessed by immunoblotting with the same antibody (Figure 1B). Alcαcyt was labeled with ^{32}P and the radioactive signal disappeared following treatment of immunoprecipitates with λPPase, indicating phosphorylation of the cytoplasmic region of Alcα.

Interestingly, membrane-associated Alcα CTF isolated from the brain is highly phosphorylated, while cytoplasmic Alcα ICD released from membrane is only partially phosphorylated (Figure 1A). This suggests that phosphorylation of Alcα and its metabolic fragments may be differentially regulated in vivo.

We next tested whether phosphorylation was involved in the interaction with KLC1, using in vitro binding assays. Alcα-FLAG and HA-KLC1 were separately expressed in N2a cells, and lysates containing Alcα-FLAG were subjected to immunoprecipitation with anti-FLAG antibody using protein G Sepharose beads. Immunoprecipitated beads were treated with or without λPPase, washed thoroughly, and combined with lysate containing HA-KLC1. After incubation, beads were collected, andwashed by centrifugation, and bound proteins (IP) and lysates were analyzed by immunoblotting with anti-HA and anti-FLAG antibodies (Figure 1C). As expected, and as reported previously (Araki *et al.*, 2007; Kawano *et al.*, 2012), HA-KLC1 was recovered through binding to bead-bound Alcα-FLAG. When beads harboring Alcα-FLAG were subjected to dephosphorylation with λPPase prior to incubation with cell lysate containing HA-KLC1, the recovery of HA-KLC1 was reduced to ~20% of that for the lysate without phosphatase treatment (Figure 1C). Decreased binding of dephosphorylated Alcα to KLC2, which is another KLC isoform expressed in neurons (Rahman *et al.*, 1998), was also observed (Figure 1D). These results indicate that phosphorylation of the Alcα cytoplasmic region is required for association with KLC.

Furthermore, this reduction was also observed for Alcγ (Figure 1E), which contains double WD motifs, as does Alcα, at least in the human protein (Araki *et al.*, 2003). In contrast, Alcβ contains only a single WD motif, and this protein showed weaker binding to KLC1, indicating a lower affinity, although the WD motif peptide of Alcβ can interact with the KLC1 TPR in vitro (see longer exposure panel of HA-KLC1 in Figure 1E; Kawano *et al.*, 2012). Regulation of the interaction with kinesin-1 by phosphorylation within the Alc cytoplasmic region is likely to be a feature of Alcα and perhaps Alcγ. Because the role of Alcα as a kinesin-1 cargo is better studied than

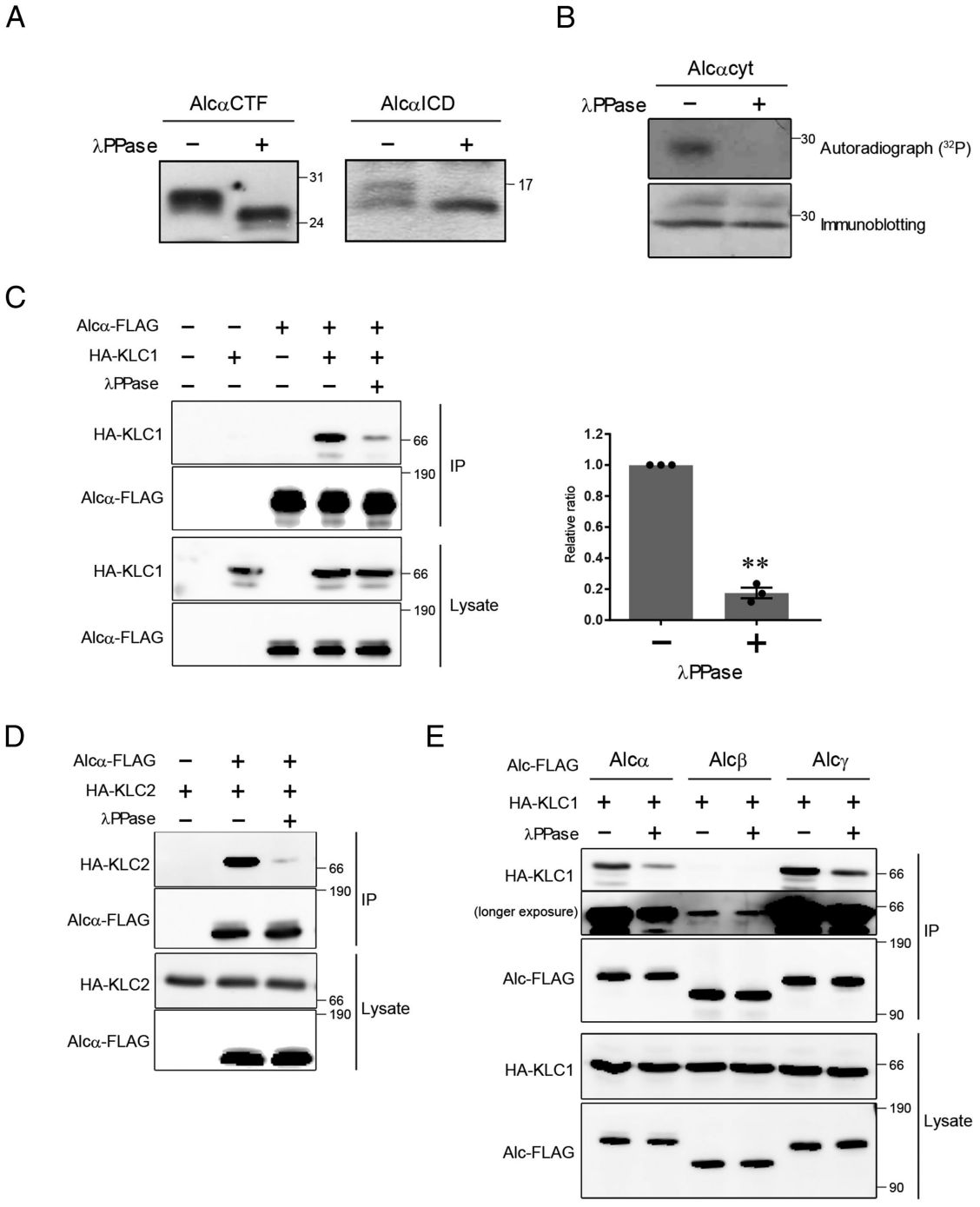

FIGURE 1: Phosphorylation of Alcadein α (Alcα) cytoplasmic region and interaction with kinesin light chain (KLC). (A) Endogenous Alcα CTF (left) and Alcα ICD (right) in mouse brain were treated with (+) or without (–) λ protein phosphatase (λPPase) and analyzed by immunoblotting with UT195 antibody. (B) HEK293 cells expressing Alcαcyt were cultured in the presence (prelabeling) or absence (immunoblotting) of [^{32}P]orthophosphate. Alcαcyt recovered by immunoprecipitation was separated by SDS–PAGE and detected by autoradiography (upper) or immunoblotting with UT83 antibody (lower). (C) In vitro binding of HA-KLC1 and Alcα-FLAG (IP) was analyzed by immunoblotting along with lysates (left). The intensities of the bands corresponding to HA-KLC1 bound to Alcα-FLAG with (+) and without (–) λPPase treatment were compared. Levels are indicated relative to the ratio without treatment (assigned a value of 1.0; right). Statistical significance was determined by Student's *t* test (means ± SE, $n = 3$, $^{**}p < 0.01$). (D) In vitro binding of HA-KLC2 and Alcα-FLAG (IP) was analyzed by immunoblotting as described in C. Experiments were performed in duplicate. (E) Alcα-FLAG, Alcβ-FLAG, and Alcγ-FLAG were separately expressed in N2a cells. The association of HA-KLC1 and Alc-FLAG proteins (IP) was analyzed by immunoblotting as described in C. The second-row panel shows the results following a longer exposure. Protein marker sizes are shown (kilodaltons).

that of Alcγ (Araki *et al.*, 2007; Kawano *et al.*, 2012), and the expression of Alcγ is lower than that of Alcα in mice (Hintsch *et al.*, 2002) and maybe in humans (Hata *et al.*, 2009), we performed further analysis to identify phosphorylation sites in the cytoplasmic domain of Alcα.

Phosphorylation within the acidic region of Alcα regulates the association with KLC1

The Alcα cytoplasmic domain, Alcα$^{871–971}$, is composed of 101 amino acids and includes many potentially phosphorylatable Ser, Thr, and Tyr residues. Five serine and threonine residues are located near the membrane region that includes the WD1 motif (residues 891–900); Thr907 and Tyr908 are located near the C-terminus of the NP sequence; eight serine and threonine residues are located within the acidic region (residues 909–957); and Ser967, Thr968, and Ser970 and Tyr971 are located in the WD2 motif (residues 962–971) (Araki *et al.*, 2003; Figure 2A).

To narrow the search for potential phosphorylation sites regulating the interaction with KLC1, we first constructed five carboxy-terminal FLAG-tagged Alcα mutants: ΔN, lacking the juxtamembrane region (residues 874–902) that includes WD1; TYAA, with Ala substituted for Thr907 and Tyr908; ΔAC, lacking the acidic region; SYAA, with Ala substitutions for Ser970 and Tyr971; and STAA, with Ala substitutions for Ser967 and Thr968 (Figure 2A). Using these mutated Alcα-FLAG proteins and the wild-type (WT) protein, the impact of λPPase treatment on the association with HA-KLC1 was examined. The ΔN, TYAA, SYAA, and STAA Alcα-FLAG mutants all showed decreased binding with HA-KLC1 following treatment with λPPase, as did the WT protein, while ΔAC Alcα-FLAG showed an equivalent ability to associate with HA-KLC1 regardless of protein phosphatase treatment (Figure 2B), indicating that phosphorylation site(s) regulating the association with KLC1 are located within the acidic region.

The acidic region is located between the two KLC-binding motifs (WD1 and WD2) and contains eight serine and threonine residues. We first confirmed phosphorylation in the acidic region using MALDI-TOF/MS. To detect phosphorylated peptides, the Alcα acidic region peptide NH_2-Met plus Alcα$^{909–950}$-FLAG peptide was expressed in N2a cells, purified from lysates using anti-FLAG antibody, and analyzed by MALDI-TOF/MS (the amino acid sequence of Alcα$^{909–950}$ is shown in the upper part of Figure 2C). Following a

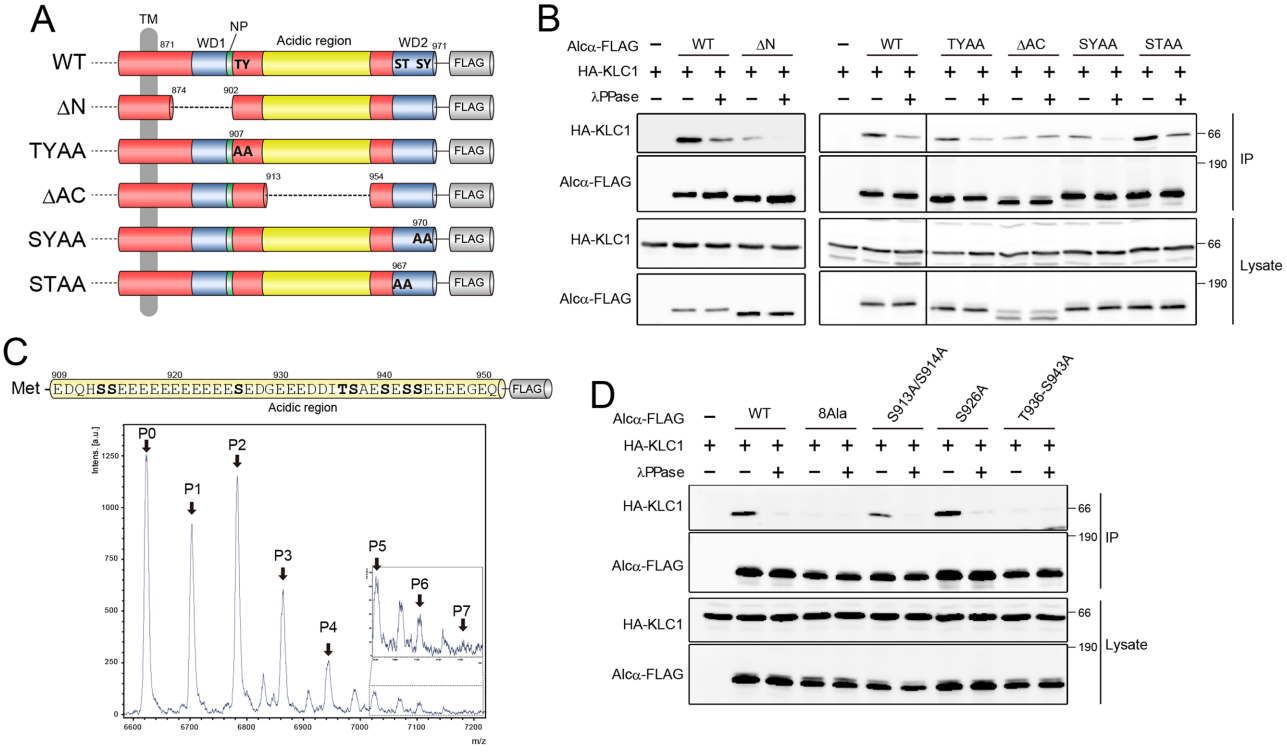

FIGURE 2: Phosphorylation of Alcα within the cytoplasmic acidic region. (A) Schematic structure of Alcα mutants used in this study. WT, wild-type Alcα; ΔN, Alcα lacking the juxtamembrane region containing WD1; TYAA, Alcα with Ala substitutions at Thr907 and Tyr908; ΔAC, Alcα lacking the acidic region; SYAA, Alcα with Ala substitutions at Ser970 and Tyr971; STAA, Alcα with Ala substitutions at Ser967 and Thr968. TM, transmembrane region. (B) Phosphatase sensitivity of indicated Alcα-FLAG proteins on the association with HA-KLC1 was examined by immunoprecipitation with lysates of N2a cells separately expressed Alcα-FLAG proteins and HA-KLC1 as described in Figure 1. (C) The carboxyl-terminal FLAG-tagged Alcα acidic region (Alcα$^{909–950}$) with an amino-terminal methionine was expressed in N2a cells and analyzed by MALDI-TOF/MS to assess phosphorylation. A representative MS spectrum is shown, and the *m/z* of phosphorylated Met+Alcα$^{909–950}$-FLAG is indicated by arrows (P1–P7) alongside the peak of nonphosphorylated peptide (P0). Areas of the spectrum that include peptides with five to seven phosphorylated amino acids are enlarged in the inset. The amino acid sequence is shown with phosphorylatable serine and threonine residues (bold letters). (D) The impact of λPPase treatment on the association with HA-KLC1 was assayed with Alcα-FLAG mutants containing alanine substitutions at the indicated serine and threonine residues within the acidic region as described in Figure 1. WT, wild-type Alcα; 8Ala, Alcα with Ala substitutions at eight serine and threonine residues; S913A/S914A, Alcα with Ala substitutions at Ser913 and Ser914; S926A, Alcα with Ala substitution at Ser926; T936-S943A, Alcα with Ala substitutions at Thr936, Ser937, Ser940, Ser942, and Ser943. Protein size markers are shown (kilodaltons).

single nonphosphorylated peptide, peptides containing from one to seven phosphorylated residues (+80 Da/phosphorylation) were detected, as shown in representative MS spectra (Figure 2C). This indicated that at least seven of the eight residues in the acidic region were phosphorylated in vivo.

To determine which serine and/or threonine residues regulate KLC1 association in a phosphorylation-dependent manner, we next constructed Alcα-FLAG mutants harboring four types of amino acid substitution and assayed the impact of λPPase treatment on the association with HA-KLC1. We prepared an Alcα-FLAG "8Ala" mutant in which all eight Ser/Thr residues were replaced with Ala, the S913A/S914A mutant, the S926A mutant, and the T936-S943A mutant with five of the Alcα$^{936–943}$ Ser/Thr residues replaced with Ala (Figure 2D). The binding of the 8Ala and T936-S943A mutants to KLC1 was lost, and as a result no effect of λPPase treatment was found. Meanwhile, the S913A/S914A and S926A mutants behaved comparably to WT Alcα-FLAG. These results indicate that phosphorylation at serine and/or threonine residues occurs within the carboxyl-terminal part of the acidic region, at Thr936, Ser937, Ser940, Ser942. or Ser943, to regulate the association with KLC1.

Multiple-site phosphorylation within the Alcα acidic region is required for strong association with KLC1

To determine which of the five residues regulates the association with KLC1, Alcα-FLAG mutants harboring single Ala substitutions (Thr936, Ser937, Ser940, Ser942, and Ser943) were generated. While replacing all five residues with Ala abrogated the impact of dephosphorylation, Alcα harboring single Ala substitutions at any of the five positions behaved comparably to WT Alcα (Figure 3A, left).

We next analyzed the interaction of KLC1 with Alcα harboring the double Ala substitutions T936/S937 and S942/S943 and the triple Ala substitution S940/S942/S943. The T936A/S937A mutant showed decreased association with KLC1 following phosphatase treatment, as did WT Alcα. The S942A/S943A double mutant also showed diminished binding to KLC1 following phosphatase treatment, but to a lesser extent than observed for the WT protein. The S940A/S942A/S943A triple mutant attenuated the association with KLC1 regardless of λPPase treatment (Figure 3A, right).

Next, we confirmed that the triple Ala substitution of Ser940, Ser942, and Ser943 attenuated the association with KLC1 in cells. Alcα-FLAG mutants harboring all eight Ala substitutions (8Ala), five Ala substitutions within the T936–S943 region (5Ala), three Ala substitutions (S940A/S942A/S943A), and two Ala substitutions (S942A/S943A) were coexpressed with HA-KLC1 and recovered by immunoprecipitation with anti-FLAG antibody as described above (Figure 3B, left). Alcα 8Ala, Alcα 5Ala, and Alcα S940A/S942A/S943A all showed significantly decreased association with HA-KLC1 compared with WT Alcα. The S942A/S943A double mutant bound to KLC1 less strongly than WT Alcα, but the decrease in binding was not significant (Figure 3B, right).

We next investigated whether the phosphorylation of Alcα at S940/S942/S943 regulates the association with KLC1 within the kinesin-1 motor. Lysates from cells expressing AlcαWT or Alcα3A together with HA-KLC1 and myc-KHC were immunoprecipitated with anti-KHC antibody. The amount of Alcα3A recovered by immunoprecipitation was decreased, even though the same amount of KLC1 was recovered (Figure 3C). We also investigated the interaction of KLC1 with a potential phosphomimetic mutant of Alcα, Alcα S940E/S942E/S943E (Alcα3E) (Supplemental Figure S1). Alcα3E associated with KLC1 at a level that was significantly less than that for AlcαWT, but that was not significantly different from that for the Alcα3A mutant. This suggests that the triple Glu substitution for Ser940, Ser942, and Ser943 does not mimic the phosphorylation state of Alcα. This may result from the fact that side chains of phosphorylated amino acids are different from acidic amino acids in terms of their chemical structure (Bah and Forman-Kay, 2016). Taken together, these results suggest that phosphorylation at three serine residues (S940, S942, and S943), located close together within the acidic region, is required for strong association with kinesin-1.

To further confirm the phosphorylation of Alcα at Ser940, Ser942, and Ser943, we attempted to prepare a phosphorylation state–specific antibody that recognizes endogenous Alcα phosphorylated at these serine residues. Antibody was raised against a peptide antigen that included phosphorylated Ser940, Ser942, and Ser943. The specificity of this phosphorylation state–specific antibody (anti-pAlcα) was examined using the corresponding Alcα Ala substitution mutants. Alcα-FLAG mutants harboring triple alanine substitutions (S940A/S942A/S943A, 3A) and single alanine substitutions (S940A, S942A, or S943A) were expressed in N2a cells along with WT Alcα-FLAG (WT), and immunoprecipitates recovered with anti-FLAG antibody were analyzed by immunoblotting using anti-pAlcα and anti-FLAG antibodies (Figure 3D). Almost the same amount of WT and the mutant proteins were detected by anti-FLAG antibody. However, only WT Alcα-FLAG (pAlcα), but not the 3A mutant, was detected using the anti-pAlcα antibody. Moreover, the anti-pAlcα antibody weakly recognized Alcα S940A (containing phosphorylatable S942 and S943 residues), Alcα S942A (containing phosphorylatable S940 and S943 residues), and Alcα S943A (containing phosphorylatable S940 and S942 residues). The pAlcα antibody therefore appears to strongly recognize Alcα phosphorylated at all three sites (Ser940, Ser942, and Ser943), but only weakly when phosphorylated at any two of the three sites.

Next, we examined phosphorylation of endogenous Alcα at Ser940, Ser942, and Ser943 in brain tissue. Alcα was recovered from mouse brain lysates by immunoprecipitation with anti-Alcα UT195 antibody, and immunoprecipitates were treated with (+) or without (-) λPPase and analyzed by immunoblotting using UT195 and pAlcα antibodies (Figure 3E). Anti-pAlcα antibody successfully detected pAlcα, and this signal disappeared following treatment with λPPase, indicating that Alcα is phosphorylated in vivo at Ser940, Ser942, and Ser943 and/or at any two of three serine residues in brain tissue.

The Ser940, Ser942, and Ser943 residues are conserved in Alcα from humans, mice/rats, and zebrafish, along with the conserved WD1 and WD2 motifs (for comparison, see Supplemental Figure S2), suggesting that phosphorylation at these serine residues is conserved in Alcα among species. We explored whether these serine residues of Alcα are conserved within the acidic region of Alcγ. There are several serine residues in the acidic region of Alcγ. Ser922 of human Alcγ, Ser917 of mouse/rat Alcγ, and Ser911 of zebrafish Alcα likely correspond to Ser940 of human Alcα, Ser950 of mouse/rat Alcα, and Ser950 of zebrafish Alcα, respectively (Supplemental Figure S2A). However, it is difficult to identify serine residues that might functionally correspond to Ser940, Ser942, and Ser943 of Alcα within the Alcγ acidic region (51% amino acid identity). Moreover, distinct from human Alcγ, the entire WD2 motif was not present in mouse/rat, suggesting that Alcγ may not play a major role as a kinesin-1 cargo receptor in mouse/rat. The WD2 motif of zebrafish Alcγ may bind KLC1 because the minimum sequence (-L/M-X-W-D/E-) for KLC-binding is retained (Kawano *et al*., 2012),

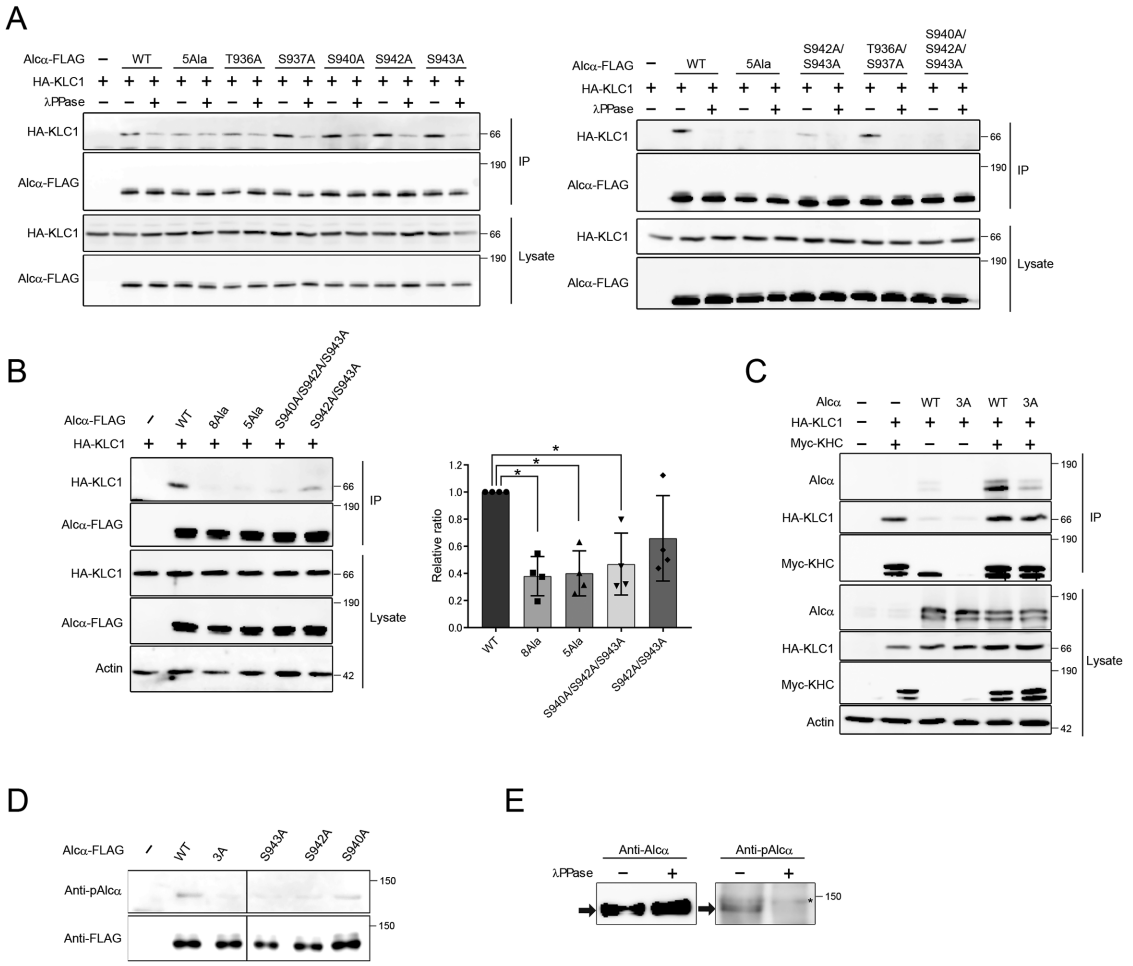

FIGURE 3: Identification of multiple phosphorylation sites. (A) The impact of λPPase treatment on the association with HA-KLC1 was assayed with Alcα-FLAG containing a single alanine substitution at Thr936, Ser937, Ser940, Ser942, or Ser943 (left), double Ser942Ala/Ser943Ala and Thr936Ala/Ser937Ala mutations, or triple Ser940Ala/Ser942Ala/Ser943Ala substitutions (right). WT Alcα-FLAG and Alcα-FLAG with five alanine substitutions (5Ala) were also tested. In vitro binding assays were performed as described in Figure 1, and representative results are shown. (B) Coimmunoprecipitation of Alcα-FLAG mutants with HA-KLC1 (left). The band intensity of bound HA-KLC1 was standardized with the band intensity of Alcα-FLAGs and levels calculated as the ratio relative to the amount bound to WT Alcα (given a value of 1; right). Statistical significance was determined by one-way analysis of variance (ANOVA) with Tukey's post hoc test (means ± SE, $n = 4$, $^*p < 0.05$). (C) WT Alcα-FLAG or Alcα3A (S940A/S942A/S943A)-FLAG was expressed in N2a cells with HA-KLC1 and myc-KHC. The immunoprecipitates with anti-KHC antibody (IP) and lysates were analyzed. Representative results are shown. (D) WT and mutant Alcα-FLAG with the indicated alanine substitutions separately expressed in N2a cells were immunoprecipitated with anti-FLAG antibody and analyzed with anti-pAlcα and anti-FLAG antibodies. Representative results are shown. (E) Alcα immunoprecipitated from mouse brain lysates were analyzed by immunoblotting with anti-Alcα UT195 and anti-pAlcα antibodies. The arrow indicates Alcα, and the asterisk indicates a nonspecific product. Protein size markers are shown (kilodaltons).

but proline residues at positions 932 and 936 in zebrafish Alcγ may alter the motif conformation to affect KLC-binding (Supplemental Figure S2A). *Caenorhabditis elegans* and *Drosophila melanogaster* have only one Alcadein gene, and the predicted proteins possess a simple WD2 motif composed of the -L-E-W-D- sequence, which is essential and a minimum sequence for KLC1-binding (Kawano *et al.*, 2012; Sanger *et al.*, 2017), and also have an obvious acidic region including serine residues that are distinct in position from the serine residues of vertebrate Alcα (Supplemental Figure S2B). Taken together, functional regulation in cargo–motor interaction by phosphorylation at serine residues within the acidic region of Alcα may have been acquired in vertebrates during evolution.

Phosphorylation of Alcα is required for proper transport of Alcα-containing vesicles

Alcα moves in axons by anterograde transport via binding and activating kinesin-1 (Kawano *et al.*, 2012). Because three phosphorylation sites are required for strong association with kinesin-1 (Figure 3C), we investigated whether phosphorylation at Ser940, Ser942, and Ser943 regulates the axonal transport of Alcα cargo. First, WT Alcα-EGFP (AlcαWT-EGFP) and Alcα-EGFP harboring S940A, S942A, and S943A mutations (Alcα3A-EGFP) were expressed in primary cultured mouse cortical neurons, and localization of Alcα was observed, along with immunostaining of MAP2B to distinguish axons from dendrites (Figure 4A). Despite decreased association with kinesin-1 (Figure 3C), signals of Alcα3A-containing

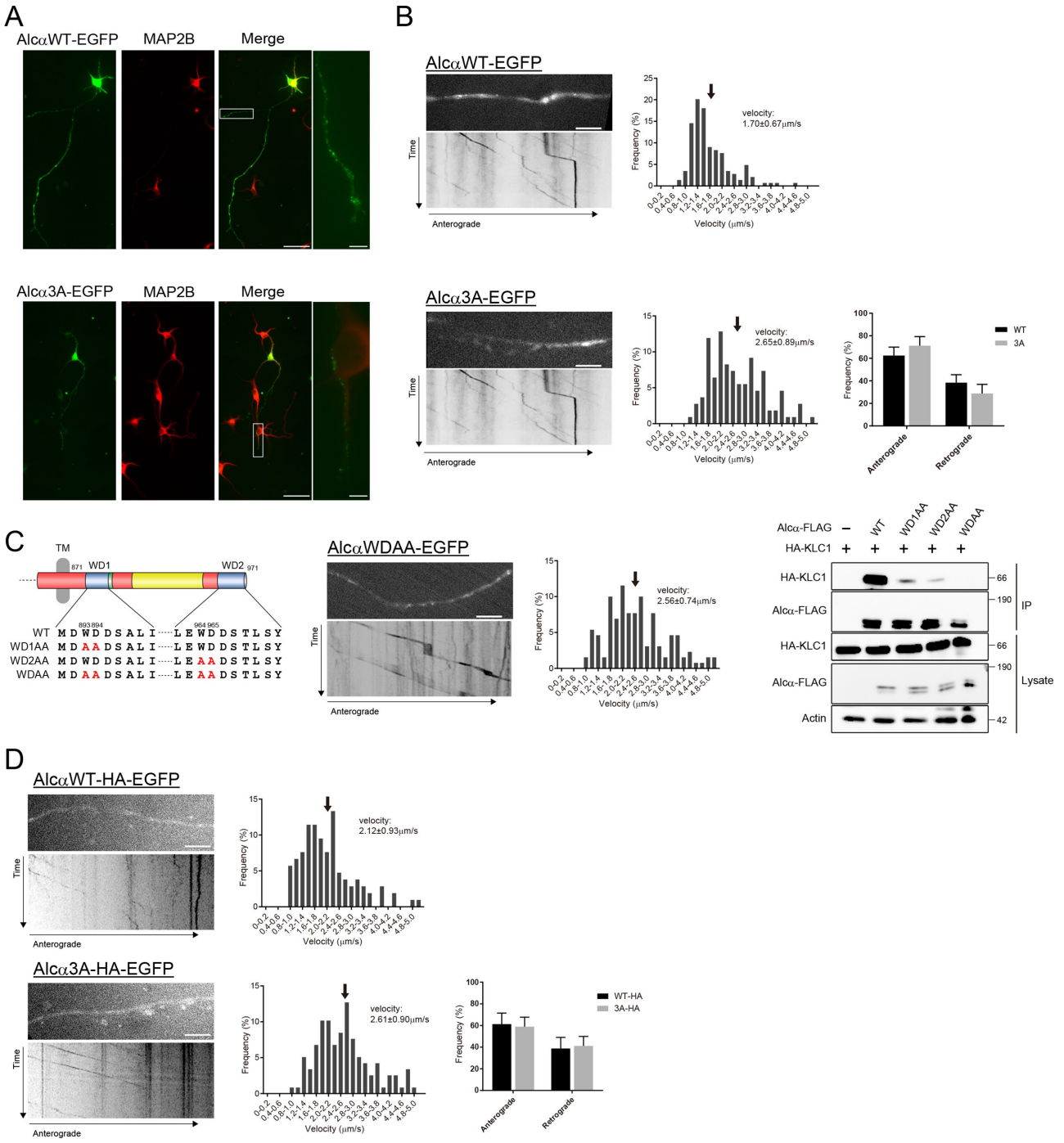

FIGURE 4: Functional analysis of the Alcα3A mutant in axonal transport by kinesin-1. (A) Primary cultured mouse cortical neurons were transfected with pcDNA3.1-AlcαWT-EGFP (upper panels) and pcDNA3.1-Alcα3A-EGFP (lower panels) at div 5. Neurons were fixed and immunostained with anti-MAP2B antibody (red) and then observed with a fluorescence microscope. Higher-magnification images of axons are shown in the panel at the far right of each set of panels. Scale bar = 50 μm and 5 μm for the higher-magnification images. (B) Primary cultured mouse cortical neurons expressing AlcαWT-EGFP (upper panels) and Alcα3A-EGFP (lower panels) were analyzed for axonal transport of Alcα cargo using a TIRF microscope. Transport of Alcα cargo is shown using movies (left upper panels; see also Supplemental Movies 1 and 2) and kymographs showing vesicle movement (left lower panels). The cumulative frequency of the velocity (middle) of the anterograde transport of Alcα cargo is shown. Data are normalized as percentages, and arrows indicate the average velocity (WT, $n = 144$; 3A, $n = 109$). Ratios for anterograde and retrograde transport of AlcαWT-EGFP (black) and Alcα3A-EGFP (gray) are shown in the panels on the right (WT, $n = 20$; 3A, $n = 21$). Statistical significance between WT and 3A was determined by Student's t test (means ± SE, not significant). (C) Primary cultured mouse cortical neurons expressing AlcαWDAA-EGFP were analyzed for axonal transport as described in B. The amino acid sequences of Alcα mutants used in this study are shown in the far left panel. A transport movie and kymograph (middle left panel; see also Supplemental Movie 3), and the cumulative frequency of the velocity (middle right) of anterograde transport are shown (data are normalized as percentages, and arrows indicate the average velocity). The

vesicles were detected in axons as well as AlcαWT (compare the upper set of panels [WT] with the lower set of panels [3A] in Figure 4A; panels on the far right show images of the boxed axonal region). This distribution indicated that Alcα3A was still transported into axons.

Next, axonal transport of Alcα vesicles was examined in living neurons using total internal reflectance fluorescence (TIRF) microscopy (Figure 4, B–D). In most known cases, impaired binding between kinesin and its cargo receptor results in disruption of the transport direction (Araki *et al.*, 2007; Vagnoni *et al.*, 2011; Chiba *et al.*, 2014a) and a decreased anterograde transport ratio in axons. However, AlcαWT-EGFP (Supplemental Movie 1) and Alcα3A-EGFP (Supplemental Movie 2) were transported in similar ratios in both anterograde and retrograde directions without significant differences (Figure 4B, left for movies and kymographs and right for direction ratios), and the ratio of stationary cargoes also did not change significantly (unpublished data). However, Alcα3A-EGFP showed a significantly higher transport velocity than that for AlcαWT-EGFP (Figure 4B, middle; $p < 0.0001$). The velocity of AlcαWT-EGFP is consistent with the in vitro kinesin-1 velocity and the velocity of transport of Alcα cargo by kinesin-1 in neurons determined previously (Kawaguchi and Ishiwata, 2000; Araki *et al.*, 2007). This higher velocity of Alcα3A-EGFP was also observed with the AlcαWDAA-EGFP mutant (Figure 4C, middle panels; Supplemental Movie 3), which does not bind to kinesin-1 because both KLC-binding WD motifs are mutated by Ala substitutions (Figure 4C, far left panel). The average velocity of AlcαWDAA-EGFP was equivalent (not significant) to that of Alcα3A-EGFP, and was significantly faster than that for AlcαWT-EGFP ($p < 0.0001$). We confirmed that AlcαWDAA-FLAG completely lost the ability to bind to HA-KLC1, while AlcαWD1AA-FLAG and AlcαWD2AA-FLAG retained reduced binding ability (Figure 4C, far right panel). Hence, it is reasonable to conclude that nonphosphorylatable Alcα3A was transported faster by a mechanism distinct from that involving direct binding to the KLC of kinesin-1.

Cytoplasmic Alcα ICD, the intracellular domain fragment of Alcα generated following cleavage by α- and γ-secretases, may influence the association of Alcα with kinesin-1, because Alcα ICD contains the KLC-interacting WD motifs. To exclude any influence of Alcα ICD on Alcα axonal transport, we analyzed axonal transport of the Alcα-HA-EGFP mutant containing the HA-tag sequence instead of the α-cleavage sequence, which is resistant to primary cleavage by α-secretase and consequently also to secondary cleavage by γ-secretase (Maruta *et al.*, 2012) (Figure 4D). Again, Alcα3A-HA-EGFP was transported with a significantly higher velocity during anterograde transport than AlcαWT-HA-EGFP ($p < 0.0001$), while the anterograde and retrograde transport ratios were almost equivalent for both AlcαWT-HA and Alcα3A-HA without any statistical significance, suggesting that this difference was not due to a change in the number of Alcα ICDs generated from AlcαWT and Alcα3A in cells. Again, the ratio of stationary cargoes did not change significantly (unpublished data). Thus, we speculated that nonphosphorylated Alcα largely lost its ability to bind kinesin-1, and this inefficient form of Alcα was instead transported by a separate axonal anterograde transport system with a velocity that is higher than that for the phosphorylation-dependent Alcα cargo mechanism.

Proper exit of Alcα cargo from Golgi requires phosphorylation of Alcα at three serine residues

We previously demonstrated the enhanced fast transport (~2.7 μm/s) of APP cargo by kinesin-1, mediated by the adaptor protein JIP1 (Chiba *et al.*, 2014a). Alcα tends to largely colocalize with APP through the neuronal adaptor protein X11-like (X11L)/Mint2 (Tomita *et al.*, 1999; Araki *et al.*, 2003), which is involved in the retention of membrane proteins in the Golgi apparatus (Zhang *et al.*, 2009; Saito *et al.*, 2011). The trend of colocalization of these proteins in the Golgi suggests that Alcα3A might be transported as APP cargo without direct binding of Alcα to kinesin-1 when X11L dissociates APP and Alcα from the ternary complex. To investigate this possibility, colocalization of Alcα-FLAG and APP in axons of mouse cortical neurons was analyzed by immunostaining using anti-FLAG and anti-APP antibodies. Some of the AlcαWT-FLAG-containing vesicles were colocalized with APP, but many vesicles were independent in axons (Figure 5A, upper set), consistent with a previous report showing that APP and Alcα are independently transported at different velocities, with only ~30% colocalized in axons in vivo (Araki *et al.*, 2007). In contrast, a smaller proportion of Alcα3A-FLAG-containing vesicles were independent from APP, and most Alcα3A-FLAG was colocalized with APP (Figure 5A, middle set), as was AlcαWDAA-FLAG (Figure 5A, lower set), which cannot bind to kinesin-1 (Figure 4C). The efficiency of colocalization was assessed, and the Pearson's correlation coefficient of Alcα-FLAG and APP was significantly higher with Alcα3A and AlcαWDAA than with AlcαWT (Figure 5B). These results strongly indicate that Alcα is not transported as typical Alcα cargo unless it is phosphorylated at the S940, S942, and S943 residues and that nonphosphorylated Alcα is instead transported as APP cargo, as are Alcα3A and AlcαWDAA mutants without the ability to bind kinesin-1.

Some KIFs, including kinesin-1, are known to mediate Golgi exit of membrane proteins (Jaulin *et al.*, 2007; Xue *et al.*, 2010b; Yin *et al.*, 2012). The missorting of Alcα3A into atypical cargo vesicles suggests that Alcα3A is unable to form functional transport vesicles at the Golgi exit point. Because X11L is believed to regulate a closed localization of Alcα and APP at Golgi (Araki *et al.*, 2004), we first confirmed that the Alcα3A mutant did not affect binding to X11L. Lysates from cells expressing Alcα3A-FLAG or AlcαWT-FLAG together with HA-X11L were subjected to coimmunoprecipitation with anti-FLAG antibody (Figure 5C). Alcα3A-FLAG and AlcαWT-FLAG recovered the same amounts of HA-X11L (Figure 5C, right), indicating that the Alcα3A mutant

inability of AlcαWDAA to bind KLC1 was shown using immunoprecipitation assays (far right panel). Alcα-FLAG with the indicated mutations in the WD motifs were coexpressed in N2a cells with HA-KLC1 and immunoprecipitated with anti-FLAG antibody (IP). A representative blot with anti-HA and anti-FLAG antibodies is shown. Protein size markers are shown (kilodaltons). (D) Primary cultured mouse cortical neurons expressing AlcαWT-HA-EGFP (upper panels) and Alcα3A-HA-EGFP (lower panels) were analyzed for axonal transport of Alcα cargo with a TIRF microscope. Transport of Alcα cargo is shown as a movie (top left panel; see also Supplemental Movies 4 and 5) and kymographs are shown in the bottom left panel. The cumulative frequency of the velocity of the anterograde transport of Alcα cargo is shown. Data are normalized as percentages, and arrows indicate the average velocity (AlcαWT-HA-EGFP, $n = 105$; Alcα3A-HA-EGFP, $n = 118$; middle panel). Ratios of anterograde and retrograde transport vesicles containing AlcαWT-HA-EGFP (black) and Alcα3A-HA-EGFP (gray) are shown in the panel on the right (AlcαWT-HA-EGFP, $n = 13$; Alcα3A-HA-EGFP, $n = 16$). Statistical significance between WT and 3A was determined by Student's *t* test (means ± SE, not significant).

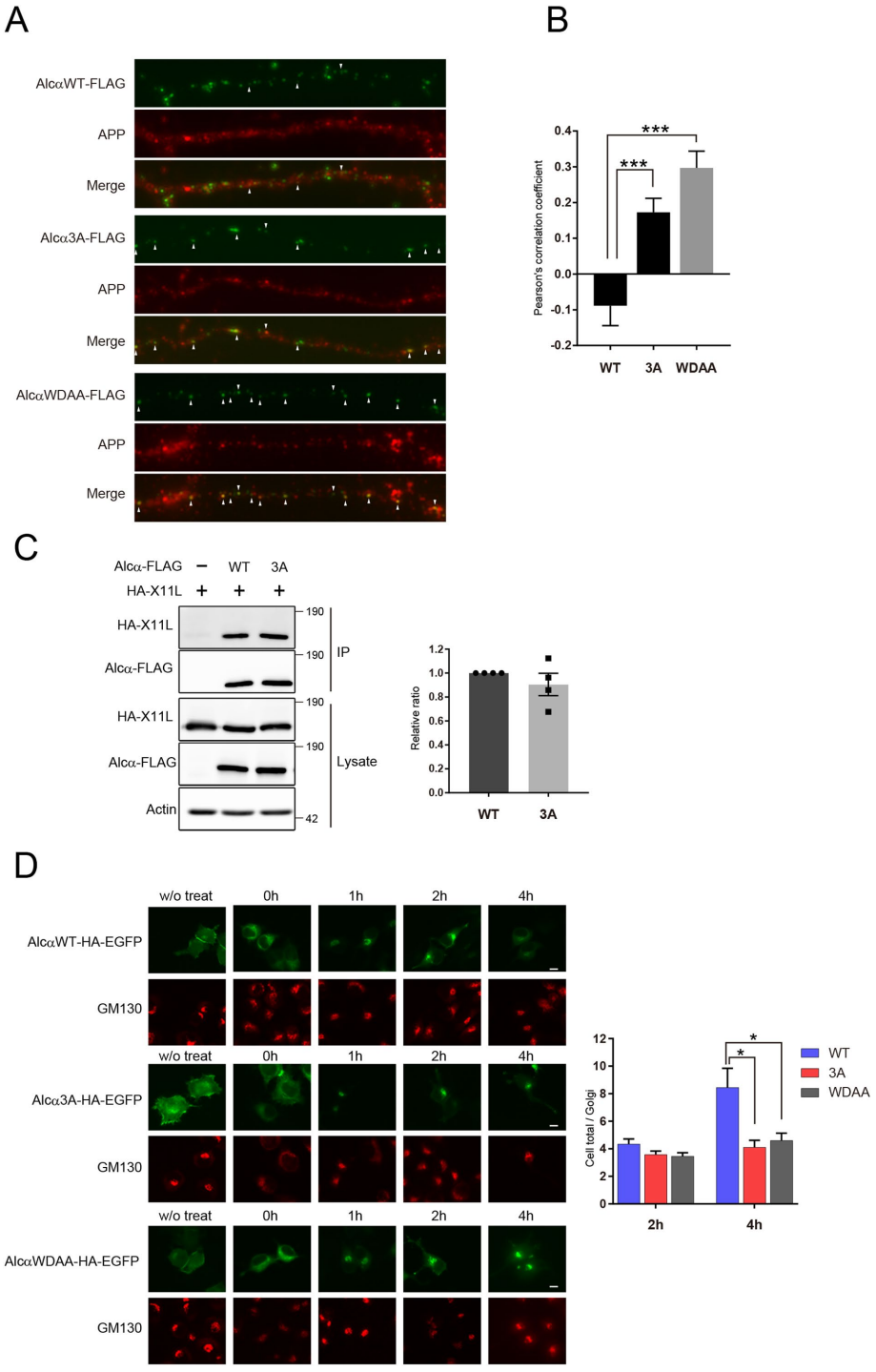

FIGURE 5: Golgi exit of Alcα cargo is regulated by the multiple-site phosphorylation. (A) Primary cultured mouse cortical neurons were transfected with pcDNA3.1-AlcαWT-FLAG (upper panels), pcDNA3.1-Alcα3A-FLAG (middle panels), or pcDNA3.1-AlcαWDAA-FLAG (lower panels) at div 5 and cultured for 8 h. Neurons were fixed and immunostained with anti-FLAG and anti-APP antibodies. Arrowheads indicate vesicles containing colocalized APP and Alcα. Scale bar = 5 μm. (B) Colocalization of axonal APP with AlcαWT-FLAG, Alcα3A-FLAG or AlcαWDAA-FLAG was calculated using the coloc2 plug-in. Pearson's colocalization coefficients are shown. Statistical significance was determined by one-way ANOVA with Tukey's post hoc test (means ± SE, WT, $n = 7$; 3A, $n = 7$; WDAA, $n = 9$; ***$p < 0.005$). (C) AlcαWT-FLAG and Alcα3A-FLAG were coexpressed in N2a cells, and immunoprecipitates with anti-FLAG antibody (IP) and lysates were analyzed by immunoblotting (left panels). The band intensity of bound HA-X11L was standardized with the band intensity of Alcα-FLAG, and the level was calculated as the ratio relative to the amount bound to WT Alcα (given a value of 1; right). Protein size markers are shown (kilodaltons). Statistical significance was determined by Student's *t* test (means ± SE, $n = 4$, not significant). (D) pcDNA3.1-AlcαWT-HA-EGFP (left upper panels), pcDNA3.1-Alcα3A-HA-EGFP (left middle panels), and pcDNA3.1-AlcαWDAA-HA-EGFP (left lower panels) were separately transfected into CAD cells. At 12 h after transfection, cells were treated with or without brefeldin A (BFA) for 4 h. After BFA was removed by changing the medium (0 h), cells were further cultured and fixed at the indicated times (0, 1, 2, and 4 h). Cells were immunostained with anti-GM130 antibody to identify the Golgi and observed using a fluorescence microscope along with the Alcα-EGFP signal. Scale bar = 10 μm. Golgi exit of Alcα was quantified by calculating the intensity of the Alcα-HA-EGFP signal within the total area of cells relative to the intensity of the Golgi area at 2 and 4 h. AlcαWT-HA-EGFP (blue; 2 h, $n = 32$; 4 h, $n = 30$), Alcα3A-HA-EGFP (red; 2 h, $n = 32$; 4 h, $n = 29$), and AlcαWDAA-HA-EGFP (gray, 2 h, $n = 32$; 4 h, $n = 23$) are shown. Statistical significance was determined by Kruskal–Wallis one-way ANOVA with Dunn's multiple comparison test (means ± SE, *$p < 0.05$).

binds to X11L as effectively as WT Alcα and suggesting that dissociation of Alcα3A from X11L is equivalent to that from WT Alcα at Golgi exit.

Finally, we examined whether kinesin-1 mediates Golgi exit of Alcα by direct binding. Again, cleavage-resistant AlcαWT-HA-EGFP, Alcα3A-HA-EGFP, and AlcαWDAA-HA-EGFP were expressed in mouse catecholaminergic CAD cells and treated with brefeldin A (BFA), which inhibits Arf GTPase, leading to the collapse of Golgi stacks. After a 4-h treatment, the medium was changed to remove BFA, and cells were cultured for a further 4 h. AlcαWT-HA-EGFP was localized in reconstructed Golgi apparatus, as observed by immunostaining with anti-GM130 antibody, and vesicular localization in peripheral cytoplasm was again evident (Figure 5D, upper panels). At 4 h after BFA treatment, both Alcα3A-HA-EGFP and AlcαWDAA-HA-EGFP, which lost all kinesin-1 binding ability, were significantly less well transported into the cell periphery, and instead remained within the Golgi (Figure 5D, left, middle and lower panels). The peripheral localization of Alcα3A-HA-EGFP and AlcαWDAA-HA-EGFP at 4 h was significantly lower than that of AlcαWT-HA-EGFP (Figure 5D, right). Taken together, the results suggest that Golgi exit of Alcα and/or proper formation of Alcα cargo is mediated by direct binding of Alcα to the KLC of kinesin-1, and this binding is dependent on multiple site phosphorylation of Alcα at Ser940, Ser942, and Ser943 residues.

DISCUSSION

Alcα and APP are major cargoes for kinesin-1 in neurons. However, the molecular mechanisms underlying how vesicles containing Alcα and APP are generated in cells, how they are associated with kinesin-1 as cargo for axonal transport, and how they are released from kinesin-1 at the nerve terminal remain to be resolved. Previous studies showed that Alcα/Clstn1 binds directly to the KLC of kinesin-1 during anterograde transport (Konecna *et al.*, 2006; Araki *et al.*, 2007), and the binding of the Alcα WD motif to the KLC1 TPR region activates kinesin-1 to initiate cargo transport (Kawano *et al.*, 2012). One study showed that replacing Ser460 of KLC1 with Ala increases the association with Clstn1, whereas replacement with Asp decreases binding to Clstn1, suggesting that phosphorylation of KLC1 at Ser460 may regulate the interaction between the cargo and kinesin-1 (Vagnoni *et al.*, 2011). Furthermore, our recent research revealed that phosphorylation of KLC1 at Thr466 regulates the velocity of transport of APP cargo by modulating the interaction with JNK-interacting protein 1b (JIP1b) (Chiba *et al.*, 2017).

We report here the following novel findings: 1) Alcα is a phosphoprotein, phosphorylation occurs within the cytoplasmic region, and the phosphorylation level is reduced following cleavage of Alcα CTF by γ-secretase to generate a cytoplasmic Alcα ICD fragment; 2) dephosphorylation of Alcα significantly decreases binding to KLC1 and KLC2; 3) phosphorylation of three amino acid residues in Alcα, Ser940, Ser942, and Ser943, is required for the association with KLC; and 4) Alcα not phosphorylated at these three serine residues is unable to form a proper cargo, and this inefficient Alcα cargo receptor is transported via distinct vesicles, likely due to the compensatory function of APP.

The Ser940, Ser942, and Ser943 phosphorylation sites are located within the acidic region of the Alcα cytoplasmic domain, between the KLC-binding WD1 and WD2 motifs. The presence of two WD motifs in a cargo molecule results in a stronger interaction with KLC than occurs with a single WD motif (Zhu *et al.*, 2012), consistent with the lower affinity of Alcβ for KLC1, which possesses only one KLC-binding WD motif. The nonphosphorylated form of Alcα harboring Ala substitutions at Ser940, Ser942, and Ser943 (Alcα3A mutant) showed significantly attenuated association with KLC. Alcα harboring double Ala substitutions at Ser942 and Ser943 (AlcαS942A/S943A mutant) also displayed diminished KLC binding, but the decrease was less than that observed for Alcα3A, indicating that multiple phosphorylation at serine residues is required for optimum association with KLC. In Alcγ, only one serine residue, Ser922 in human Alcγ, is conserved, and this Ser922 may correspond to Ser940 of human Alcα (Supplemental Figure S2). Although it remains uncertain whether Ser922 of Alcγ is phosphorylated, phosphorylation of Ser922 and/or other Ser/Thr residues within the acidic region may regulate KLC binding.

Phosphorylation within the acidic region may change the conformation or alter the disordered structure of the Alcα cytoplasmic region that includes the two WD motifs, because regulation of disordered structure by phosphorylation has been reported for other proteins (Iakoucheva *et al.*, 2004; Travers *et al.*, 2015). The protein kinase(s) responsible for phosphorylating Ser940, Ser942, and Ser943 of Alcα remain unknown. However, casein kinase I (CK1) and/or II (CK2) are probable candidates. CK1 and 2 are known to phosphorylate serine residues embedded in acidic regions of DARPP-32 in neurons (Desdouits *et al.*, 1995), and our in vitro experiments showed that at least CK2 can phosphorylate a substrate peptide containing these serine residues (unpublished observation by YS).

We expected that axonal transport of the Alcα3A mutant may be impaired, because this mutant was almost incapable of binding to kinesin-1. However, Alcα3A vesicles were observed in axons, and their transport velocity was higher than that of WT Alcα vesicles. Further experiments revealed that Alcα3A was included in distinct APP cargo vesicles. Although previous observations suggested that APP and Alcα work cooperatively during Golgi exit (Ludwig *et al.*, 2009; Takei *et al.*, 2015), the transport of Alcα cargo vesicles is largely competitive with and independent of APP cargo vesicles after Golgi exit (Araki *et al.*, 2007). APP cargoes are transported at a higher velocity than Alcα cargoes in neuronal axons, even though both cargoes are transported by the same kinesin-1 molecular motor (Araki *et al.*, 2007; Chiba *et al.*, 2014a). Additionally, endogenous Alcα cargoes are transported separately from APP cargoes, and colocalization of the two cargoes in axons is ~30% at most (Araki *et al.*, 2007). However, in the present study, we showed that inefficient binding of Alcα to kinesin-1 results in increased colocalization within APP vesicles in axons. This nonconventional localization of Alcα is presumably due to the compensatory action of APP cargo in defective Alcα transport.

Interestingly, the Alcα3A mutant displayed decreased Golgi exit of Alcα vesicles in undifferentiated CAD cells, which exhibit lower expression of endogenous APP than in neurons (Fragkouli *et al.*, 2017). Several reports suggest that KIFs such as kinesin-1 play an important role in Golgi exit of cargo vesicles and/or post-Golgi transport of cargoes (Jaulin *et al.*, 2007; Xue *et al.*, 2010b; Yin *et al.*, 2012). KIFs may function to form tubular structures at the Golgi exit point (reviewed in Weisz and Rodriguez-Boulan, 2009). Our finding that the Alcα3A mutant decreases Golgi exit is consistent with the previous report on KIF function and suggests that Alcα3A is unable to form proper Alcα cargoes. Although the exit of Alcα3A or AlcαWDAA from Golgi was decreased, vesicles containing these mutants were still transported in axons, albeit by alternative vesicles and at a higher velocity. These results indicate that decreased binding to kinesin-1 impairs the proper formation of Alcα vesicles at the Golgi, and defective Alcα is incorporated into distinct APP cargo vesicles and possibly others.

Alcα vesicles can carry various cargo proteins, but when Alcα is not phosphorylated, these cargoes will not be transported efficiently to the required destination. Although relatively little is known about the roles of Alcα transport vesicles, the phenotypes of Alcα gene knockout animals have been reported. Axon branching is impaired in zebrafish, and spine formation is affected in mice (Ponomareva *et al.*, 2014; Ster *et al.*, 2014). Impaired phosphorylation of Alcα might cause these phenotypes in vivo, but this requires further investigation.

Taken together, our findings allow us to hypothesize that Alcα recruits and strongly binds kinesin-1 following multiple site phosphorylation of serine residues in its cytoplasmic acidic region, which facilitates the formation of tubular membrane structures that include Alcα and its cargo functionally associated with kinesin-1 (Figure 6). Although our results do not directly demonstrate whether Alcα located in the Golgi is highly phosphorylated, they revealed that WT Alcα binds strongly to kinesin-1, unlike the Alcα mutant harboring alanine substitutions at Ser940, Ser942, and Ser943, and confirmed that endogenous Alcα is phosphorylated at these multiple serine residues, which regulates binding to kinesin-1. Prior to the association of phosphorylated Alcα with kinesin-1, Alcα and APP are thought to dissociate from a ternary complex including X11L by an unknown mechanism (Figure 6). One possible regulatory process in the release of APP from X11L may be the phosphorylation of X11L (Sakuma *et al.*, 2009). However, it is not known if phosphorylation of X11L contributes to release of Alcα. Nevertheless, the present

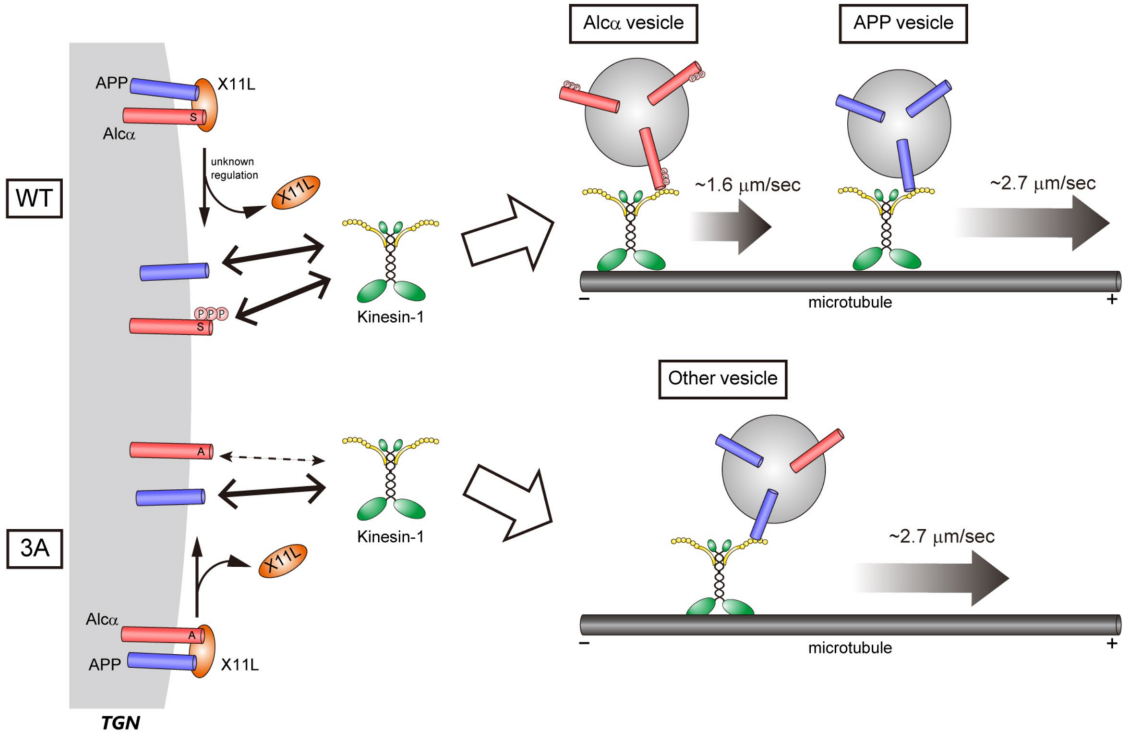

FIGURE 6: Role of Alcα phosphorylation in Golgi exit of Alcα vesicles by kinesin-1. Schematic representation of the possible regulation of Alcα vesicle formation and transport by phosphorylation of Alcα at Ser940, Ser942, and Ser943 is shown. Alcα and APP are thought to colocalize in the Golgi by binding to X11L, and both membrane proteins dissociate from X11L by an unknown mechanism but still reside close to each other in the Golgi. Alcα residing at the Golgi is phosphorylated at three serine residues within the cytoplasmic acidic region that is located between the WD1 and WD2 motifs. This phosphorylation enhances the association with kinesin-1 and the formation of vesicles containing Alcα. The resultant Alcα vesicles are transported in an anterograde manner by kinesin-1 at the correct velocity (~1.6 μm/s) for proper Alcα cargo, in which Alcα is functionally associated with kinesin-1 (upper panel). APP vesicles are also formed independently and transported in an anterograde manner by kinesin-1 at the correct velocity (~2.7 μm/s) for proper APP cargo. When Alcα is not phosphorylated at the three phosphorylatable serine residues (due to substitution with alanine), the resultant inefficient Alcα cannot bind kinesin-1 and fails to exit from the Golgi by forming its own cargo. However, some Alcα does manage to exit from the Golgi following incorporation into other vesicles containing APP cargo. When Alcα is included in APP cargo vesicles, the resultant vesicles are transported by APP-associated kinesin-1 in an anterograde manner at a higher velocity (lower panel; enhanced fast transport velocity of ~2.7 μm/s) that is more typical of APP cargo transport by kinesin-1 (Chiba *et al.*, 2014a).

findings broaden our understanding of the function and regulation of cargo–motor protein interactions and provide insight into the mechanism of proper cargo formation.

MATERIALS AND METHODS

Antibodies

Rabbit polyclonal anti-Alcα UT195 antibody was raised to the same antigen as was used to generate UT83 (described previously in Araki *et al.*, 2003). A polyclonal phosphorylation state-specific anti-pAlcα antibody was raised against the antigen peptide NH_2-Ala-Glu-pSer-Glu-pSer-pSer-Glu-Glu-Glu-Lys-Lys+Cys-$CONH_2$. Further information can be found in the Supplemental Methods Appendix.

Plasmids

The original plasmids pcDNA3 and pcDNA3.1 containing Alcα and Alcα ICD were described previously (Araki *et al.*, 2007). These were mutated using PCR and subcloned into pcDNA3.1. Details of plasmid construction are described in the Supplemental Methods Appendix.

Prelabeling of cells

HEK293 cells expressing the cytoplasmic region of Alcα (Alcα$^{871–971}$/Alcαcyt) were labeled for 3 h at 37°C with [^{32}P]orthophosphate as described previously (Suzuki *et al.*, 1994). Alcαcyt was immunoprecipitated and incubated with or without ≥400 units of lambda protein phosphatase (λPPase; P9614; Sigma-Aldrich) and analyzed by autoradiography followed by Tris-glycine–buffered SDS–PAGE. A detailed description of the procedures can be found in the Supplemental Methods Appendix.

Detection of phosphorylated Alcα, Alcα CTF, and Alcα ICD in mouse brain

For detection of endogenously generated Alcα CTF and Alcα ICD (Figure 1A), subfractionation of mouse brain lysate was performed as described (Nakaya and Suzuki, 2006) and analyzed by immunoblotting followed by Tris-tricine–buffered SDS–PAGE using 10% (wt/vol for Alcα CTF) and 17.5% (wt/vol for Alcα ICD) polyacrylamide gels (Schägger, 2006). A detailed description of the procedures can be found in the Supplemental Methods Appendix.

Cell culture and primary cultured neurons

Cell culture and transfection are described in the Supplemental Methods Appendix.

Primary cultures of mouse cortical neurons were prepared and cultured as described previously (Chiba *et al.*, 2014a). All animal studies were conducted in compliance with the guidelines of the Animal Studies Committee of Hokkaido University.

Binding assay for Alcα-FLAG and HA-KLC1

N2a cells were transfected with pcDNA3.1-Alcα-FLAG or pcDNA3.1-HA-KLC1 plasmid and cultured for 24 h. Cells were lysed in HBS-T buffer. Cell lysates containing Alcα-FLAG were subject to immunoprecipitation with anti-FLAG M2 antibody and protein G Sepharose beads (GE Healthcare Bio-Sciences, Little Chalfont, UK), and immunoprecipitates were treated with or without λPPase (≥200 U) at 30°C for 3 h. Beads were washed and then combined with cell lysate containing HA-KLC1 and incubated with rotation. Immunoreactive proteins were quantified using an LAS-4000 mini (Fujifilm, Tokyo, Japan).

Immunofluorescence microscopy analysis and quantification of fluorescence intensity

At 12 h after transfection, CAD cells were treated with 2 μg/ml brefeldin A (BFA) for 4 h. After washing with medium containing 100 μg/ml cycloheximide, cells were further incubated for the indicated time and immunostained with anti-GM130 antibody. Primary cultured mouse cortical neurons (in vitro, day 5) were transfected with plasmids by the calcium phosphate method and cultured for 8 h. Cells were fixed and immunostained with indicated antibodies. Fluorescence images were acquired with a fluorescence microscope (BZ-710X; Keyence, Osaka, Japan), and quantitative analysis and colocalization efficiency were analyzed with Fiji/ImageJ and the Colco2 Fiji plug-in (ImageJ-Fiji-ImgLib; http://Fiji.sc or http://imageJ.net).

Total internal reflectance fluorescence/TIRF microscopy analysis

At in vitro day 4 (div 4), primary cultured mouse cortical neurons were transfected with plasmids and cultured for 16 h. The cells were observed using a TIRF microscopy system (C1; Nikon, Tokyo, Japan) with a charge-coupled device camera (Cascade 650; Photometrics) in an incubation chamber supplied with 5% CO_2 at 37°C. The velocity of anterograde transport was analyzed quantitatively as described in the Supplemental Information of a previous report (Araki *et al.*, 2007). The average velocity (indicated with an arrow in the histograms) ± SD is shown. Statistical analysis of cargo velocity distributions was performed using the Kruskal–Wallis test followed by Dunn's multiple comparisons test or Mann–Whitney tests. Kymographs of moving vesicles were assembled using KymoMaker (Chiba *et al.*, 2014b). The direction of moving vesicles was further followed by residual analysis. The proportion (percentage) of anterograde and retrograde vesicles relative to the indicated total number of vesicles is shown as the frequency, as described previously (Araki *et al.*, 2007).

ACKNOWLEDGMENTS

We thank George S. Bloom (University of Virginia) and Sam Gandy (Mount Sinai School of Medicine) for the kind supply of antibodies. This work was supported in part by Grants-in-Aid for JSPS Research Fellow 16J04020 to Y.S. and 15J02220 to K.C. and Grants-in-Aid for Scientific Research 15K18854 to S.H. and 262930110 and 16K14690 to T.S. from the Ministry of Education, Culture, Sports, Science and Technology (MEXT) in Japan, by National Institutes of Health Grant AG047270 to A.C.N., by the Strategic Research Program for Brain Sciences from the Japan Agency for Medical Research and Development (16dm0107142h0001, 17dm0107142h0002), and by a Grant-in-Aid for Scientific Research on Innovative Areas—Platforms for Advanced Technologies and Research Resources "Advanced Bioimaging Support" to T.S.

REFERENCES

Araki Y, Kawano T, Taru H, Saito Y, Wada S, Miyamoto K, Kobayashi H, Ishikawa HO, Oshsugi Y, Yamamoto T, *et al.* (2007). The novel cargo Alcadein induces vesicle association of kinesin-1 motor components and activates axonal transport. EMBO J 26, 1475–1486.

Araki Y, Miyagi N, Kato N, Yoshida T, Wada S, Nishimura M, Komano H, Yamamoto T, De Strooper B, Yamamoto K, Suzuki T (2004). Coordinated metabolism of Alcadein and amyloid β-protein precursor regulates FE65-dependent gene transactivation. J Biol Chem 279, 24343–24354.

Araki Y, Tomita S, Yamaguchi H, Miyagi N, Sumioka A, Kirino Y, Suzuki T (2003). Novel cadherin-related membrane proteins, Alcadeins, enhance the X11-like protein mediated stabilization of amyloid β-protein precursor metabolism. J Biol Chem 278, 49448–49458.

Bah A., Forman-Kay JD (2016). Modulation of intrinsically disordered protein function by post-translational modifications. J Biol Chem 291, 6696–6705.

Boraxbekk CJ, Ames D, Kochan NA, Lee T, Thalamuthu A, Wen W, Armstrong NJ, Kwok JB, Schofield PR, Reppenmund S, *et al.* (2015). Investigating the influence of KIBRA and CLSTN2 genetic polymorphisms on cross-sectional and longitudinal measures of memory performance and hippocampal volume in order individuals. Neuropsychologia 78, 10–17.

Chiba K, Araseki M, Nozawa K, Furukori K, Araki Y, Matsushima T, Nakaya T, Hata S, Saito Y, Uchida S, *et al.* (2014a). Quantitative analysis of APP axonal transport in neurons—role of JIP1 in APP anterograde transport. Mol Biol Cell 25, 3569–3580.

Chiba K, Chien K, Sobu Y, Hata S, Kato S, Nakaya T, Okada Y, Nairn AC, Kinjo M, Taru H, *et al.* (2017). Phosphorylation of KLC1 modifies interaction with JIP1 and abolishes the enhanced fast velocity of APP transport by kinesin-1. Mol Biol Cell 28, 3857–3869.

Chiba K, Shimada Y, Kinjo M, Suzuki T, Uchida S (2014b). Simple and direct assembly of kymographs from movies with Kymomaker. Traffic 15, 1–11.

Chua JJ, Butkevich E, Worseck JM, Kittelmann M, Gronborg M, Behrmann E, Stelzl U, Pavlos NJ, Lalowski MM, Eimer S, *et al.* (2012). Phosphorylation-regulated axonal dependent transport of syntaxin 1 is mediated by a kinesin-1 adapter. Proc Natl Acad Sci USA 109, 5862–5867.

Desdouits F, Cohen D, Nairn AC, Greengard P, Girault J-A (1995). Phosphorylation of DARPP-32, a dopamine- and cAMP-regulated phosphoprotein, by casein kinase I in vitro and in vivo. J Biol Chem 270, 8772–8778.

Dodding MP, Mitter R, Humphries AC, Way M (2011). A kinesin-1 binding motif in vaccinia virus that is widespread throughout the human genome. EMBO J 30, 4523–4538.

Fragkouli A, Koukouraki P, Vlachos IS, Paraskevopoulou MD, Harzigeorgiou AG, Doxakis E (2017). Neuronal ELAVL proteins utilize AUF-1 as a co-partner to induce neuron-specific alternative splicing of APP. Sci Rep 7, 44507.

Fu MM, Holzbaur EL (2013). JIP1 regulates the directionality of APP axonal transport by coordinating kinesin and dynein motors. J Cell Biol 202, 495–508.

Hata S, Fujishige S, Araki Y, Kato N, Araseki M, Nishimura M, Hartmann D, Saftig P, Fahrenholz F, Taniguchi M, *et al.* (2009). Alcadein cleavages by APP α- and γ-secretases generate small peptides p3-Alcs indicating Alzheimer disease-related γ-secretase dysfunction. J Biol Chem 284, 36024–36033.

Hata S, Fujishige S, Araki Y, Taniguchi M, Urakami K, Peskind E, Akatsu H, Araseki M, Yamamoto K, Martins N R, *et al.* (2011). Alternative γ-secretase processing of γ-secretase substrates in common forms of mild cognitive impairment and Alzheimer disease: evidence for γ-secretase dysfunction. Ann Neurol 69, 1026–1031.

Hata S, Taniguchi M, Piao Y, Ikeuchi T, Fagan AM, Holzman DM, Bateman R, Sohrabi HR, Martins RN, Gandy S, *et al.* (2012). Multiple γ-secretase product peptides are coordinately increased in concentration in the CSF of a subpopulation of sporadic Alzheimer's disease subjects. Mol Neurodegen 7, 16.

Hintsch G, Zurlinden A, Meskenaite V, Steuble M, Fink-Widmer K, Kinter J, Sonderegger P (2002). The calsyntenins: a family of postsynaptic membrane proteins with distinct neuronal expression patterns. Mol Cell Neurosci 21, 393–409.

Hirokawa N, Niwa S, Tanaka Y (2010). Molecular motors in neurons: transport mechanisms and roles in brain function, development, and disease. Neuron 68, 610–638.
Iakoucheva LM, Radivojac P, Brown CJ, O'Connor TR, Sikes JG, Obradovic Z, Dunker K (2004). The importance of intrinsic disorder for protein phosphorylation. Nucleic Acids Res 32, 1037–1049.
Jaulin F, Xue X, Rodriguez-Boulan E, Kreitzer G (2007). Polarization-dependent selective transport to the apical membrane by KIF5B in MDCK cells. Dev Cell 13, 511–522.
Kamal A, Stokin GB, Yang Z, Xia CH, Goldstein LS (2000). Axonal transport of amyloid precursor protein is mediated by direct binding to the kinesin light chain subunit of kinesin-I. Neuron 28, 449–459.
Kamogawa K, Kohara K, Tabara Y, Takita R, Miki T, Konno T, Hata S, Suzuki T (2012). Utility of plasma levels of soluble p3-Alcadeinα as a biomarker for sporadic Alzheimer's disease. J Alzheimer Dis 31, 421–428.
Kawaguchi K, Ishikata S (2000). Temperature dependence of force, velocity, and processivity of single kinesin molecules. Biochem Biophys Res Commun 272, 895–899.
Kawano T, Araseki M, Araki Y, Kinjo M, Yamamoto T, Suzuki T (2012). A small peptide sequence is sufficient for initiating kinesin-1 activation through part of TPR region of KLC1. Traffic 13, 834–848.
Konecna A, Frischnech R, Kinter J, Ludwig A, Steuble M, Meskenaite V, Indermuhle M, Engrl M, Cen C, Mateos JM, *et al*. (2006). Calsyntenin-1 docks vesicular cargo to kinesin-1. Mol Biol Cell 17, 3651–3663.
Konno T, Hata S, Hamada Y, Horikoshi-Sakuraba Y, Nakaya T, Saito Y, Yamamoto T, Yamamoto T, Maeda M, Ikeuchi T, *et al*. (2011). Coordinate increase of γ-secretase reaction products in the plasma of some female Japanese sporadic Alzheimer's disease patients: quantitative analysis with a new ELISA system. Mol Neurodegen 6, 76.
Koo EH, Sisodia SS, Archer DR, Martin LJ, Weidemann A, Beyreuther K, Fisher P, Masters CL, Price DL (1990). Precursor of amyloid protein in Alzheimer disease undergoes fast anterograde axonal transport. Proc Natl Acad Sci USA 87, 1561–1565.
Lipina TV, Parsad T, Yokomaku D, Luo L, Connor SA, Kawabe H, Wang YT, Brose N, Roder JC, Craig AM (2016). Cognitive deficits in calsyntenin-2-deficient mice associated with reduced GABAergic transmission. Neuropsychopharmacol 41, 802–810.
Ludwig A, Blume J, Diep TM, Yuan J, Mateos JM, Leuthauser K, Steuble M, Streit P, Sonderegger P (2009). Calsyntenins mediate TGN exit of APP in a kinesin-1-dependent manner. Traffic 10, 572–589.
Maruta C, Saito Y, Hata S, Gotoh N, Suzuki T, Yamamoto T (2012). Constitutive cleavage of the single-pass transmembrane protein Alcadeinα prevents aberrant peripheral retention of kinesin-1. PLoS One 7, e43058.
Nakaya T, Suzuki T (2006). Role of APP phosphorylation in FE65-dependent gene transactivation mediated by AICD. Genes Cells 11, 633645.
Omori C, Kaneko M, Nakajima E, Akatsu H, Waragai M, Maeda M, Moroshima-Kawashima M, Saito Y, Nakaya T, Taru H, *et al*. (2014). Increased levels of plasma p3-Alcα35, a major fragment of Alcadeinα by γ-secretase cleavage, in Alzheimer's disease. J Alzheimers Dis 39, 861–870.
Pettem KL, Yokomaku D, Luo L, Linhoff MW, Prasad T, Connor SA, Siddiqui TJ, Kawabe H, Chen F, Zhang L, *et al*. (2013). The specific α-neurexin interactor calsyntenin-3 promotes excitatory and inhibitory synapse development. Neuron 80, 113–128.
Piao Y, Kimura A, Urano S, Saito Y, Taru H, Yamamoto T, Hata S, Suzuki T (2013). Mechanism of intramembrane cleavage of Alcadeins by γ-secretase. PLoS One 8, e62431.
Ponomareva OY, Holmen IC, Sperry AJ, Eliceriri KW, Halloran MC (2014). Calsyntenin-1 regulates axon branching and endosomal trafficking during sensory neuron development in vivo. J Neurosci 34, 9235–9248.
Rahman A, Friedman DS, Goldstein LS (1998). Two kinesin light chain genes in mice. Identification and characterization of the encoded proteins. J Biol Chem 273, 15395–15403.
Saito Y, Akiyama M, Araki Y, Sumioka A, Shiono M, Taru H, Nakaya T, Yamamoto T, Suzuki T (2011). Intracellular trafficking of the amyloid β-protein precursor (APP). regulated by novel function of X11-like. PLoS One 6, e22108.
Sakuma M, Tanaka E, Taru H, Tomita S, Gandy S, Nairn AC, Nakaya T, Yamamoto T, Suzuki T (2009). Phosphorylation of the amino-terminal region of X11L regulates its interaction with APP. J Neurochem 109, 465–475.
Sanger A, Yip YY, Randall TS, Pernigo S, Steiner RA, Dodding MP (2017). SKIP controls lysosome positioning using a composite kinesin-1 heavy and light chain-binding domain. J Cell Sci 130, 1637–1651.
Schägger H (2006). Tricine-SDS–PAGE. Nat Protocols 1, 16–22.
Ster J, Stuble M, Orlando C, Diep TM, Akhmedov A, Raineteau O, Pernet V, Sonderegger P, Gerber U (2014). Calsyntenin-1 regulates targeting of dendritic NMDA receptors and dendritic spine maturation in CA1 hippocampal pyramidal cells during postnatal development. J Neurosci 34, 8716–8727.
Suzuki T, Oishi M, Marshak DR, Czernik AJ, Nairn AC, Greengard P (1994). Cell cycle-dependent regulation of the phosphorylation and metabolism of the Alzheimer amyloid precursor protein. EMBO J 13, 1114–1122.
Takei N, Sobu Y, Kimura A, Urano S, Piao Y, Araki Y, Taru H, Yamamoto T, Hata S, Nakaya T, Suzuki T (2015). Cytoplasmic fragment of Alcadeinα generated by regulated intramembrane proteolysis enhances APP transport into the late-secretory pathway and facilitates APP cleavage. J Biol Chem 290, 987–995.
Tomita S, Ozaki T, Taru H, Oguchi S, Takeda S, Yagi Y, Sakiyama S, Kirino Y, Suzuki T (1999). Interaction of a neuron-specific protein containing PDZ domains with Alzheimer's amyloid precursor protein. J Biol Chem 274, 2243–2254.
Travers T, Shao H, Joughin BA, Douglas A, Lauffenburger DA, Wells A, Camacho CJ (2015). Tandem phosphorylation within an intrinsically disordered region regulates ACTN4 function. Sci Sig 8, ra51.
Um JW, Paramanik G, Ko JS, Song YM, Lee D, Kim H, Park KS, Sudhof TC, Tabuchi K, Ko J (2014). Calsyntenins function as synaptogenic adhesion molecules in concert with neurexins. Cell Rep 27, 1096–1109.
Vagnoni A, Perkinton MS, Gray EH, Francis PT, Noble W, Miller CC (2011). Calsyntenin-1 mediates axonal transport of the amyloid precursor protein and regulates Aβ production. Hum Mol Genet 21, 2845–2854.
Vale RD, Reese T, Sheetz MP (1985). Identification of a novel force-generating protein, kinesin, involved in microtubule-based motility. Cell 42, 39–50.
Verhey KJ, Hammond JW (2009). Traffic control: regulation of kinesin motors. Nat Rev Mol Cell Biol 10, 765–777.
Verhey KJ, Lizotte DL, Abramson T, Barenboin L, Schnapp BJ, Rappoport TA (1998). Light chain-dependent regulation of kinesin's interaction with microtubules. J Cell Biol 143, 1053–1066.
Verhey KJ, Meyer D, Deehan R, Blenis J, Schnapp BJ, Rapoport TA, Margolis B (2001). Cargo of kinesin identified as JIP scaffolding proteins and associated signaling molecules. J Cell Biol 152, 959–970.
Wang LZ, Chen F, Tong H, Reddy MV, Luo L, Seshadrinathan S, Zhang L, Holthauzen LM, Craig AM, Ren G, Rudenko G (2014). Calsyntenin-3 molecular architecture and interaction with neurexin 1α. J Biol Chem 289, 34530–34542.
Weisz OA, Rodriguez-Boulan E (2009). Apical trafficking in epithelial cells: signals, clusters and motors. J Cell Sci 122, 4253–4266.
Wobst H, Schmitz B, Schachner M, Diestel S, Leshchyns'ka I, Sytnyk S (2015). Kinesin-1 promotes post-Golgi trafficking of NCAM140 and NCAM180 to the cell surface. J Cell Sci 128, 2816–2829.
Xu J., Reddy BJ, Anand P, Shu Z, Cermelli S, Mattson MK, Tripathy SK, Hoss MT, James NS, King SJ, *et al*. (2012). Casein kinase 2 reverses tail-independent inactivation of kinesin-1. Nat Commun 3, 754.
Xue B, Dumbrack RL, Williams RW, Dunker AK, Uversky VN (2010a). PONDR-FIT: A meta-predictor of intrinsically disordered amino acids. Biochim Biophys Acta 1804, 996–1010.
Xue X, Jaulin F, Espenel C, Kreitzer G (2010b). PH-domain-dependent selective transport of p75 by kinesin-3 family motors in non-polarized MDCK cells. J Cell Sci 123, 1732–1741.
Yin X, Feng X, Takei Y, Hirokawa N (2012). Regulation of NMDA receptor transport: aKIF17-cargo binding/releaseing underlies synaptic plasticity and memory in vivo. J Neurosci 18, 5486–5499.
Yip YY, Permigo S, Sanger A, Xu M, Parsons M, Steiner RA, Dodding MP (2016). The light chains of kinesin-1 are autoinhibited. Proc Natl Acad Sci USA 113, 2418–2423 .
Zhang Y, Wang Y-G, Zhang Q, Liu X-J, Liu X, Jiao L, Zhu W, Zhang Z-H, Zhao X-L, He C (2009). Interaction of Mint2 with TrkA is involved in regulation of nerve growth factor-induced neurrites outgrowth. J Biol Chem 284, 12469–12479.
Zhu H, Lee HY, Tong Y, Hong BS, Kim KP, Shen Y, Lim KJ, Mackenzie F, Tempel W, Park HW (2012). Crystal structures of the tetratricopeptide repeat domains of kinesin light chains: insight into cargo recognition mechanisms. PLoS One 7, e33943.